

**LIFETIME OF  $^{16}\text{O}$ -RICH OXYGEN ISOTOPE RESERVOIR IN THE SOLAR NEBULA.**

T. Ushikubo<sup>1</sup>, T. J. Tenner<sup>1</sup>, H. Hiyagon<sup>2</sup>, and N. T. Kita<sup>1</sup>, <sup>1</sup>Department of Geoscience, University of Wisconsin-Madison, Madison, WI 53706, USA (ushi@geology.wisc.edu), <sup>2</sup>Department of Earth and Planetary Science, University of Tokyo, Tokyo, 113-0033, Japan.

**Introduction:** The temporal and spatial variations of oxygen isotope ratios of the Solar Nebula are important constraints for the early Solar system evolution and precursors of solid materials [e.g. 1]. Recently, we reported that chondrules from primitive carbonaceous chondrites preserve oxygen isotope ratios when they formed [2,3]. This suggests that CAIs in the same meteorites also preserve their intrinsic oxygen isotope ratios. We report new oxygen isotope ratios and Al-Mg systematics for CAIs and AOAs from primitive carbonaceous chondrites, Acfer 094 and Y 81020 [4].

**Samples and Methods:** Oxygen isotope ratios of 1 Fluffy Type A (FTA) CAI (E8) from Y 81020 (CO3.0), 3 FTA (G16, G49, G104) and 2 fine-grained (G5:Melilite-rich, G92:Anorthite-rich) CAIs, and 4 Amoeboid Olivine Aggregates (AOAs) (G17, G28, G44, G58) from Acfer 094 (C-ungroup3.0) were measured by the Cameca IMS-1280 ion microprobe at UW-Madison. Because of small size (250 to 600  $\mu\text{m}$  in size) and fine-grained texture of the samples, a small  $\text{Cs}^+$  primary beam ( $\sim 3 \mu\text{m}$ ,  $\sim 25 \text{pA}$ ) was used. Analytical conditions were similar to those of [5]. Typical 2 SD errors of  $\delta^{18}\text{O}$ ,  $\delta^{17}\text{O}$ , and  $\Delta^{17}\text{O}$  ( $=\delta^{17}\text{O} - 0.52 \times \delta^{18}\text{O}$ ) are  $\pm 0.8$ ,  $\pm 1.1$ , and  $\pm 1.1 \text{‰}$ , respectively.

Magnesium isotope ratios of melilite of all CAIs (4 FTA and 2 fine-grained) were measured with a small  $\text{O}^+$  primary beam ( $\sim 5 \mu\text{m}$ ,  $\sim 50 \text{pA}$ ). Analysis were also made for anorthite in 2 CAIs (G16, G92; Figure 1). Analytical conditions were similar to those of [6]. As preliminary estimates, inferred initial  $^{26}\text{Al}/^{27}\text{Al}$  ratios,  $(^{26}\text{Al}/^{27}\text{Al})_0$ , of CAIs were determined by regression data through the origin of the Al-Mg isochron diagram ( $\delta^{26}\text{Mg}^*=0$  at  $^{27}\text{Al}/^{24}\text{Mg}=0$ ).

**Results and Discussion:**

*Oxygen isotope ratios of CAIs and AOAs.* We obtained 52 oxygen isotope data from multiple phases (melilite, spinel, Ca-rich pyroxene, anorthite, and olivine) of CAIs and AOAs. Oxygen isotope ratios of the all samples are  $^{16}\text{O}$ -rich ( $\Delta^{17}\text{O} \sim -22$  to  $-24 \text{‰}$ ) and distributed near the CCAM line [7] and the PCM line, which is determined by oxygen isotope data of chondrules from Acfer 094 [6] (Figure 2). Two exceptions are melilite near an altered area and also the matrix of E8 ( $\Delta^{17}\text{O} \sim -14.3$  and  $-6.9$ , respectively). Because mass-dependent fractionations of Mg isotopes of these CAIs are small ( $-0.3 \pm 0.6$  to  $1.1 \pm 0.4 \text{‰/amu}$ ), oxygen isotope fractionation by evaporation can be negligible

if evaporative loss occurred after condensation of the precursor of CAIs [8,9].

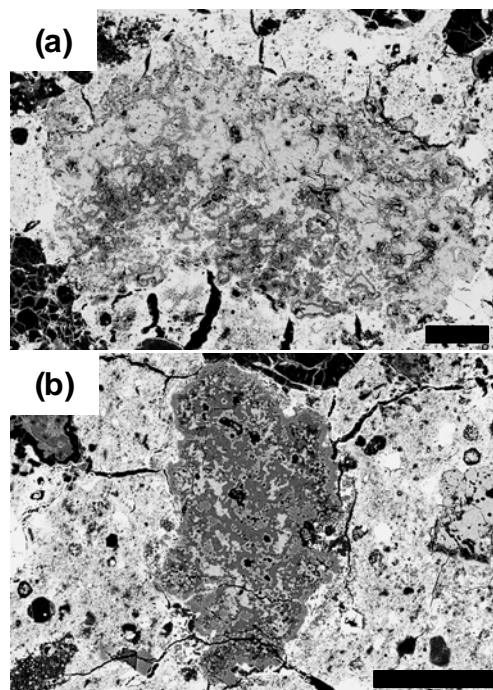


Figure 1. Back scattered electron images of CAIs (a) G16 (FTA) and (b) G92 (An-rich) from Acfer 094. Scale bars indicate 100 $\mu\text{m}$ .

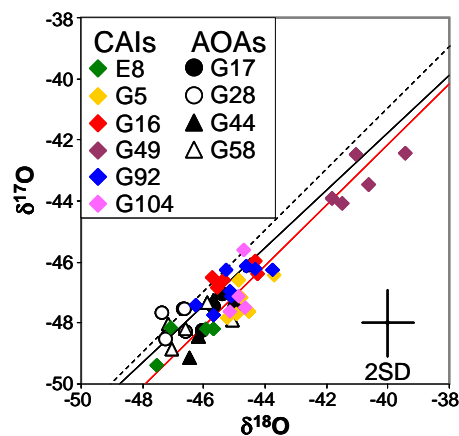


Figure 2. Oxygen isotope ratios of CAIs and AOAs. Two measurements of E8, melilite near alteration and matrix, are not shown. Reference lines are the CCAM (black) [7], Young and Russell (dotted) [10], and PCM (red) [11] lines, respectively. Typical reproducibility (2SD) of analyses are also shown.

*Al-Mg systematics of CAIs.* We obtained multiple Mg isotope data for each CAI (n=2 to 9) to calculate isochrones (e.g. Figure 3). Values of MSWD of isochrones are from 0.54 (G16) to 2.5 (G49). The inferred  $(^{26}\text{Al}/^{27}\text{Al})_0$  of CAIs are mostly between  $4 \times 10^{-5}$  and  $5.0 \times 10^{-5}$  (Figure 4) and slightly lower than the canonical value ( $\sim 5.2 \times 10^{-5}$ ) that is determined by CAIs from CV chondrites [12,13]. One exception is anorthite in G92 with a significantly lower value of  $\sim 5.4 \times 10^{-6}$  (Figure 3). Anorthite in G16 and G92 occurs between pyroxene-rim and melilite and the  $^{27}\text{Al}/^{24}\text{Mg}$  ratios of anorthite in these two CAIs ( $\sim 700$  to  $\sim 1570$ ) are higher than those of anorthite in chondrules from Acfer 094 (27 to 55) [6] or “igneous” coarse-grained CAIs (typically 100 to 600) [e.g. 14,15]. High  $^{27}\text{Al}/^{24}\text{Mg}$  ratios of anorthite may be caused by a reaction between pre-existing refractory minerals and nebular gas [16], but not by the crystallization of anorthite from melt.

*Evidence for  $^{16}\text{O}$ -rich reservoir at the time of chondrule formation.* Figure 4 summarizes results of this study. All CAIs and AOAs have  $^{16}\text{O}$ -rich oxygen isotope ratios. This is consistent with oxygen isotope ratios of pristine CAIs from other carbonaceous chondrites [17]. Although we do not find any evidence for multiple heating processes in these CAIs (G92 may be an exception), the inferred  $(^{26}\text{Al}/^{27}\text{Al})_0$  of these CAIs are lower than those of pristine CAIs in CV chondrites [12,13]. This indicates either 1) heterogeneity of  $^{26}\text{Al}$  abundance ( $\sim 10\%$ ) in the Solar Nebula, 2) later formation of CAIs in Acfer 094 relative to CV chondrites, or 3) size dependence of residence time of CAIs in the Solar Nebula [18].

The low inferred  $(^{26}\text{Al}/^{27}\text{Al})_0$  value of anorthite in G92 suggests that anorthite formed at  $\sim 2.3$  Myrs after the oldest CAIs, which is around the same time as chondrule formation (Figure 4). Assuming reaction with nebular gas for anorthite formation [16] of G92, nebular gas that reacted with G92 should have been  $^{16}\text{O}$ -rich at the time of anorthite formation. No ferro-magnesian minerals, similar to those found in chondrules, are observed along the outer edge of the Ca-pyroxene rim of G92, implying that anorthite formation must have occurred in an environment distinct from those of chondrule formation. One possible explanation is that the anorthite formation of G92 occurred outside of a dust-enriched layer where chondrules formed and the oxygen isotope ratio of ambient gas was  $^{16}\text{O}$ -rich. Another explanation is that the interaction between G92 (solid) and ambient gas (possibly SiO+O) caused mass independent isotope fractionation [19], although this model would likely need to be confirmed experimentally.

**References:** [1] Yurimoto H. et al. (2007) in Protoplastars and Planets V, pp.849-862. [2] Ushikubo T. et

al. (2009) *LPS XL*, Abstract #1383. [3] Tenner T. J. et al. (2011) *LPS XLII*, Abstract#1426. [4] Kimura M. et al. (2008) *MAPS*, 43, 1161-1177. [5] Nakamura T. et al. (2008) *Science*, 321, 1664-1667. [6] Ushikubo T. et al. (2010) *LPS XLI*, Abstract #1491. [7] Clayton R. N. et al. (1977) *EPSL*, 34, 209-224. [8] Grossman L. et al. (2000) *GCA*, 64, 2879-2894. [9] Wang J. et al. (2001) *GCA*, 65, 479-494. [10] Young E. D. and Russell S. S. (1998) *Science*, 282, 1874-1877. [11] Ushikubo et al. (2011) *LPS XLII*, Abstract #1183. [12] Jacobsen B. et al. (2009) *EPSL*, 272, 353-364. [13] MacPherson G. J. et al. (2010) *ApJ*, 711, L117-L121. [14] Podosek F. A. et al. (1991) *GCA*, 55, 1083-1110. [15] Goswami J. N. et al. (1994) *GCA*, 58, 431-447. [16] Krot A. N. et al. (2004) *MAPS*, 39, 1517-1553. [17] Krot A. N. et al. (2010) *ApJ*, 713, 1159-1166. [18] Ciesla F. J. (2009) *Icarus*, 200, 655-671. [19] Marcus R. A. (2004) *J. Chem. Phys.*, 121, 8201-8211.

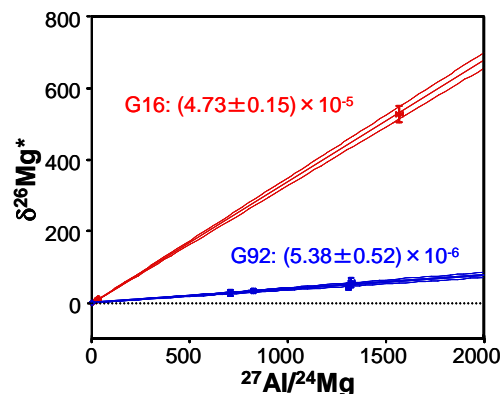


Figure 3. The Al-Mg systematics of G16 and G92. Note that we assume  $\delta^{26}\text{Mg}^*=0$  at  $^{27}\text{Al}/^{24}\text{Mg}=0$  to calculate regression lines. Errors are 95% confidence level.

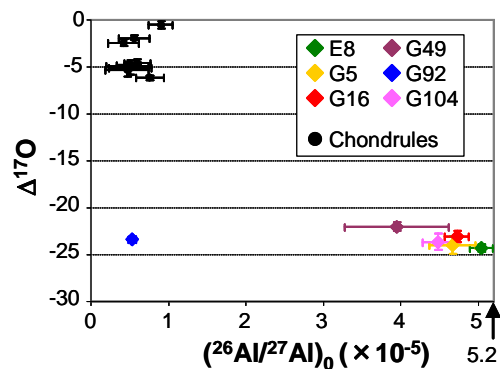


Figure 4. The  $\Delta^{17}\text{O}$  and  $(^{26}\text{Al}/^{27}\text{Al})_0$  plot of CAIs. Data of chondrules from Acfer 094 [2] are also shown for comparison. Errors are 95% confidence level.